Tight junction formation in early Xenopus laevis embryos: identification and ultrastructural characterization of junctional crests and junctional vesicles

Cardellini, Pietro; Cirelli, Alessandro; Citi, Sandra

Cell Tissue Res (2007) 330:247–256
DOI 10.1007/s00441-007-0472-9

REGULAR ARTICLE

Tight junction formation in early *Xenopus laevis* embryos: identification and ultrastructural characterization of junctional crests and junctional vesicles

Pietro Cardellini · Alessandro Cirelli · Sandra Citi

Received: 25 June 2007 / Accepted: 12 July 2007 / Published online: 4 September 2007

Abstract How tight junctions (TJ) form during early amphibian embryogenesis is still an open question. We used time-lapse video microscopy, scanning electron microscopy (SEM), TEM and freeze-fracture to gain new insight into TJ biogenesis in early clevages of *Xenopus laevis*. Video analysis suggests three phases in junction formation between blastomeres. A first "waiting" phase, where new unpigmented lateral membranes are generated. A second "mixing" phase, where the unpigmented lateral membrane is separated from the pigmented apical membrane by an area showing a limited degree of intermingling of cortical pigment. And a third "sealing" phase, characterized by the formation of cingulin-containing boundaries between membrane domains, and their rapid directional adhesion in a zipper-like fashion. By SEM, we characterized these boundaries ("junctional crests", JC) as arrays of villiform protrusions at the border between old and new membranes. In the 2-cell embryo, JC are deeply located, and thus not visible at the surface, but they become increasingly more superficial as cleavages progress. After adjacent blastomeres have adhered to each other, fractured JC display linear arrays of junctional vesicles (JV) of 1–3 μm diameter. TEM analysis shows that JV are symmetrically located near the apposed membranes of adjacent blastomeres, and that the membranes near the JV display focal sites of intimate contact, typical of TJ. Freeze-fracture analysis confirms that intramembrane fibrils, typical of TJ, are present at adhesion sites. We conclude that TJ are formed following the sealing of JC, through the recruitment, sorting and assembly of membrane and cytoplasmic proteins at or near JV.

Keywords Tight junction · Electron microscopy · Membrane vesicle · Cingulin · *Xenopus laevis* (Anura)

Funding: We thank the Italian Ministry for University and Scientific Research, the Swiss League against Cancer, the Swiss National Fonds, and the State of Geneva for financial support. We thank Laurent Guillemot for comments on the manuscript.

P. Cardellini · A. Cirelli · S. Citi
Department of Biology, University of Padua,
Padua, Italy

S. Citi (✉)
Department of Molecular Biology, University of Geneva,
Geneva, Switzerland
e-mail: sandra.citi@molbio.unige.ch

Introduction

Tight junctions (TJ) are regions of intimate contact between the apicolateral membranes of vertebrate epithelial cells, which create a continuous seal between adjacent cells, thereby controlling the flow of ions and solutes through the space between cells ("barrier" function). In addition, TJ define the boundary between the apical and basolateral domains of the plasma membrane ("fence" function). By freeze-fracture electron microscopy, TJ are characterized by the presence of fibrils and corresponding grooves (Goodenough and Revel 1970), which appear in sections as focal sites of close apposition of adjacent plasma membranes ("kisses") (Farquhar and Palade 1963).

How TJ are assembled is an important question, which is related to how epithelial cells differentiate, establish apico-basal polarity, and form epithelial tissues. In early *Xenopus laevis* embryos, the formation of TJ is a prerequisite for the establishment of the blastocoel, the internal cavity whose molecular composition is distinct from the outside environment. The timing of TJ assembly in *Xenopus* embryos has been the object of some controversy. Early electrophysiological studies suggested that TJ formation occurred only at the 64-cell stage (Palmer and Slack 1970). However, measure-

ment of the sensitivity of membrane potentials to variations in extracellular concentrations of sodium and potassium indicated that functional TJ are formed after the first cell division (Slack and Warner 1973). In addition, 2-cell embryos are impermeable to the passage of tracers (Kalt 1971b) and display a separation between old and new membranes (Bluemink 1971; Sanders and Zalik 1972; Byers and Armstrong 1986), indicating the presence of both barrier and fence functions at this stage. Finally, the cytoplasmic TJ protein cingulin accumulates at the boundary between old apical membrane and new lateral membrane in 2-cell embryos (Cardellini et al. 1996), indicating that the cytoplasmic backbone of TJ is assembled at the 2-cell stage. Although this evidence indicates that functional TJ are present in 2-cell embryos, continuous fibrils imaged by freeze-fracture electron microscopy have not been observed before the 8-cell stage (Sanders and DiCaprio 1976; Cardellini and Rasotto 1988), suggesting that complete maturation of TJ, with the polymerization of the constituent transmembrane proteins (claudins; Tsukita et al. 2001) into stable fibrils, may be technically difficult to image.

In contrast to cingulin (Cardellini et al. 1996) and atypical protein kinase C (Chalmers et al. 2003), which are recruited into nascent TJ from maternal pools which are associated with the apical cortex, the TJ-associated proteins ZO-1 and occludin are assembled into nascent junctions following insertion of two distinct populations of membrane vesicles into the new lateral membrane (Fesenko et al. 2000). Thus, TJ form as the result of the concerted assembly of molecules, from both apical and lateral membrane domains, into a specific area at the border between these domains. However, the dynamics of formation of such a site, and its ultrastructure remain unclear.

To address this issue, we used time-lapse video microscopy, SEM, TEM and freeze-fracture analysis of early *Xenopus* embryos. The results indicate that TJ are formed following the sealing of "junctional crests" (JC) that appear at the border between new and old membranes, and are characterized by villiform protrusions on the membrane surface, and junctional vesicles (JV) in the submembrane cytoplasm.

Materials and methods

Embryos

Pairs of *Xenopus laevis* were injected with chorionic gonadotropin (Serono Profasi HP5000). Males were injected with 300 I.U. of hormone 36 h and 12 h before coupling. Females were injected with 100 I.U. and 400 I.U. 36 h and 12 h before coupling, respectively. Embryos were dejellied by treatment with 165 mM L-cysteine in double-distilled water adjusted to pH 8.9, and reared in MMR/4 (25 mM NaCl, 0.5 mM KCl, 0.5 mM $CaCl_2$, 0.25 mM $MgCl_2$, 1.25 mM HEPES, pH 7.4), and different developmental stages were processed for microscopy. To separate cell–cell junctions, embryos were placed in MMR/4 lacking calcium. Whole-mount immunoperoxidase labeling of embryos with anti-cingulin antiserum was carried out as described in Cardellini et al. (1996).

Time-lapse video microscopy

For time-lapse video microscopy, embryos were imaged using a Olympus SZH dissecting microscope, equipped with a JVC TK-C1380E camcorder connected to a JVC BR9060E video recorder. Frames were obtained each 3.2 sec or 6.4 sec, resulting in a final acceleration of 80× and 160×, respectively.

Scanning electron microscopy (SEM)

For SEM, embryos were fixed in 2.5% glutaraldehyde, 100 mM sodium cacodylate (pH 7.2) for 2 h at room temperature. After fixation, embryos were washed four times (10 min each) with 100 mM sodium cacodylate. Embryos were then postfixed in 1% osmium tetroxide (1 h), washed in cacodylate buffer, and dehydrated in ethanol at 4°C. Samples were then further dehydrated with a Critical Point apparatus, whereby ethanol was gradually substituted by liquid carbon dioxide at 4°C. Carbon dioxide was then evaporated at 40°C, and embryos were cleaved to allow observation of inner blastomere membranes. The material was then coated with a gold conducting layer (1–1.5 μm thick) in an Edwards S. 150 B evaporator, at a pressure of 10^{-1} atm. Samples were observed and imaged using a Cambzone Stereoscan 260 microscope. For each developmental stage, between 3 and 8 embryos where mechanical separation resulted in clear blastomere cleavage were observed by SEM.

Transmission electron microscopy (TEM) and freeze-fracture

Embryos were fixed, washed and dehydrated in ethanol as described above. They were then incubated in propylene oxide (twice for 10 min at room temperature), followed by propylene oxide and Epon epoxy resin (1:1, 1 h at 45°C), and finally Epon resin (1 h at 37°C). Embryos were mounted in silicone moulds, and the resin was polymerized for 24 h at 37°C, 24 h at 45°C, and 24 h at 60°C. Sections were obtained with a LKB UltrotomeIII. Semithin sections were stained with toluidine blue (1%), and observed by light microscopy. Thin sections were stained with uranyl acetate and lead citrate, and observed with a Hitachi H600 microscope.

For freeze-fracture electron microscopy, 8-cell embryos were processed as described in Cardellini and Rasotto (1988).

Results

Dynamics of junction formation during early cleavages of *Xenopus laevis* embryos

We used time-lapse video microscopy to examine membrane dynamics and junction formation during the first cleavages of *Xenopus laevis* embryos. The egg displays an animal/vegetal polarity axis, with the vegetal pole, rich in yolk platelets, at the bottom. The first cleavage plane is vertical, and defines the dorso-ventral axis. The cleavage furrow appears as a deepening of the plasma membrane within the animal pole (Fig. 1a) as a result of the contraction of the subcortical actomyosin ring. The second division axis is perpendicular to the first and separates the two dorsal blastomeres, which show a less pigmented cortex, from the two ventral blastomeres (Fig. 1b). The third division plane is asymmetrically positioned towards the animal pole and becomes

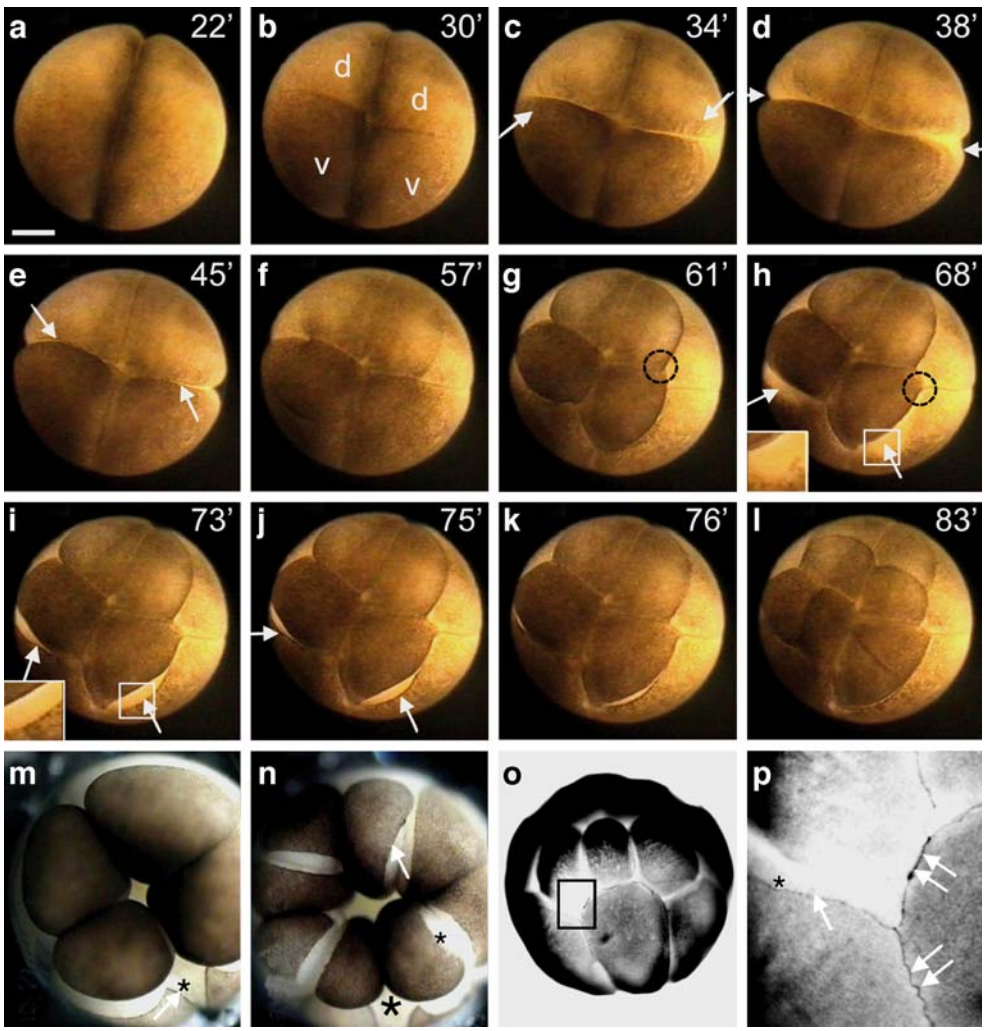

Fig. 1 Dynamics of first cleavages of *Xenopus* embryos. **a**–**l** Still images captured from a time-lapse video recording of a cleaving embryo, under normal calcium conditions. Time in minutes (') is indicated on the upper right corner, taking as starting time (0') the beginning of cleavage. **m**, **n** Embryo cleaving in medium with low calcium. **o**, **p** Whole embryo immunostained with anti-cingulin antiserum (**o**), and higher magnification detail [(**p**)=*boxed area* in (o)]. (*d*) and (*v*) in **b** indicate dorsal and ventral blastomeres, respectively. *Arrows* in **c** indicate membrane folds generated by the pulling force of the cleavage furrow. *Arrows* in **d** and **h** indicate junctional membranes in the "mixing" phase at the 4-cell and 8-cell stage embryo, respectively. *Arrows* in **e**, **i**, **j** and **n** indicate JC. The *insets* in **h** and **i** show magnified images of the corresponding *boxed areas*, to visualize better the emergence of the JC (**i**) following the "mixing" phase (**h**). Note how the JC in **j** is progressively zippered along its length in **k** and **l**, and how sealing hides the less pigmented new membrane below the junction. *Circles* in **g** and **h** indicate "triple points", e.g. tricellular contacts where sealing of newly formed JC starts. *Asterisks* in **m**, **n** and **p** indicate new lateral membrane, devoid of pigment. *Arrows* in **p** indicate immunolabeling for cingulin, which accumulates at the border between old and new membrane either in sealed JC (*double arrows*) or in yet unsealed JC (*single arrow*). *Bar* **a** 200 μm

apparent as a focal deepening of the membrane, which intersects the junctions resulting from the first and second cell division (Fig. 1f–g).

As the cleavage furrow deepens and separates new blastomeres during each division, new lateral membrane is generated by the exocytic insertion of membrane vesicles into the plasma membrane (Kalt 1971a; Sanders and Singal 1975; Byers and Armstrong 1986). The old apical membrane can be distinguished from the new lateral membrane because the apical domain is pigmented, whereas the lateral domain lacks pigment granules. Based on the pigmentation of the plasma membranes exposed on the surface of the cleaving embryo, we identified three phases in the formation of junctions between new blastomeres. These phases were more clearly visible starting from the third cell division, since in the first two cleavages newly formed junctions are located in a more recessed, internal position (see Fig. 2). During the first phase ("waiting"), which lasts for about 12–15 min (out of the 21–25 min of the cell cycle), the new unpigmented membranes, which have been formed following cell division, remain separated, and are only partially visible at the surface (arrows in Fig. 1d–h). The next phase ("mixing") is very rapid, and consists of the formation of an area of membrane where the superficial material and pigment granules from apical and lateral sides appear intermingled, so that the border between the external pigmented membranes and the new lateral membranes is not sharply defined (arrows in Fig. 1h, magnified area in inset). The third phase ("sealing") begins with the appearance of sharply defined, darker lines, which separate lateral from apical membranes (arrows in Fig. 1i–j, magnified area in inset in Fig. 1i). We call these structures "junctional crests" (JC). The sealing is completed when the two JC of adjacent blastomeres fuse together in a directional zipper-like fashion, starting from the side closer to the junction generated by the previous division, towards the opposite end (compare Fig. 1j–k). The sites where zippering up of adjacent JC begins are tricellular contacts ("triple points", circles in Fig. 1g–h), where the new junction intersects the junction formed during the previous cell division. There is always a slight stagger between the position of the JC on the two opposing sides of the pre-existing junction, so that a perfect cross is never formed, and only three, but not four blastomeres converge into the same "triple" point (dotted circles in Fig. 1g–h).

Once the JC are sealed, the new lateral membrane is no longer visible at the surface, since it is located below the sealed JC (Fig. 1l). However, if embryos are reared in a medium with a low calcium concentration, the adhesive function of cadherins is inhibited, and the JC fail to seal (arrows in Fig. 1m–n). Under these conditions, the new lateral membrane remains readily visible on the outer surface (asterisks in Fig. 1m–n). Immunostaining of

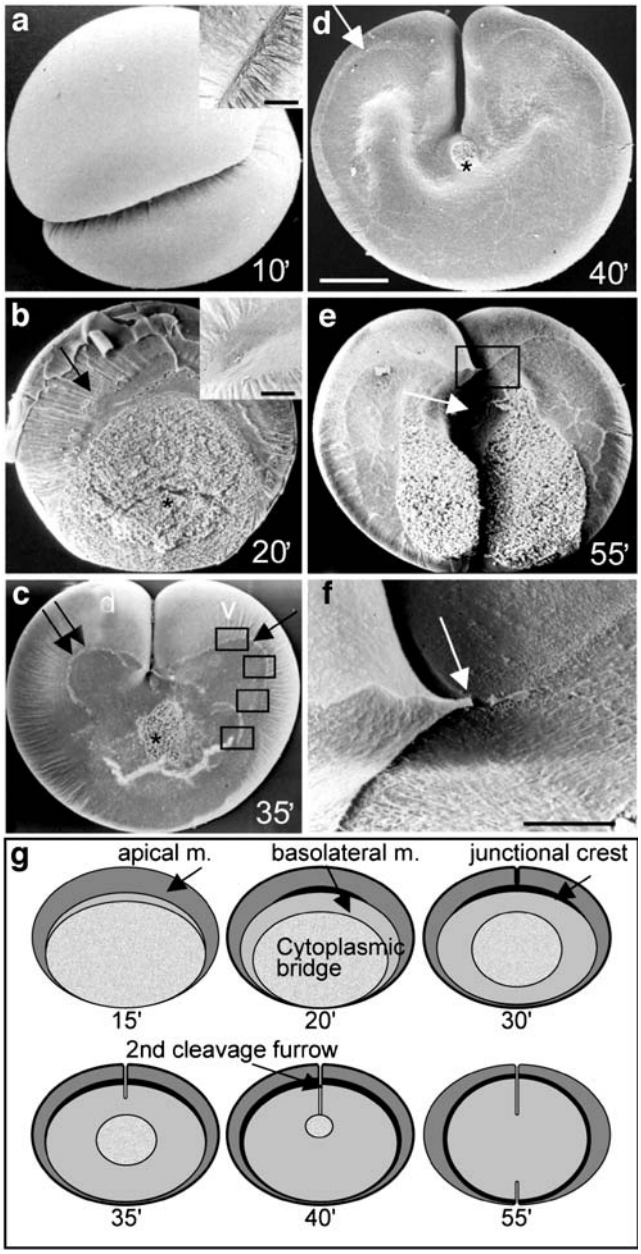

Fig. 2 Scanning electron microscopy analysis of *Xenopus* embryos during early cleavage. **a** Image of a whole embryo undergoing the first cleavage. **b–f** Inner surfaces of half-embryos (obtained by fracturing away one of the two blastomeres at the 2-cell stage) undergoing the first (**b**) and the second (**c–f**) cell division. **f** Higher magnification detail of the *boxed area* in **e**. *Insets* in **a** and **b** show higher magnifications of the cleavage furrow. **g** Schematic diagram of the dynamics of JC formation (see text for description). The *asterisks* in **b**, **c** and **d** indicate the cytoplasmic bridge linking dividing blastomeres. In **e** the fracture was along the second plane of division, thus the bridges between dorsal and ventral blastomeres are seen. *Double arrows* and *arrow* in **c** indicate the JC on the dorsal and ventral sides, respectively. *Rectangles* along the ventral JC in **c** show the areas which are magnified in Fig. 3a–d. *Arrow* in **e** indicates the blastocoel. *Arrow* in **f** indicates a "triple point". Note in **c** that the JC is detected on both dorsal (*d*) and ventral (*v*) sides, but it extends deeper into the embryo in the ventral side, possibly due to the asymmetric position of the nuclei, and/or to the higher fluidity of the ventral cytoplasm. *Bar* **a–e** 200 μm, **f** 80 μm, *insets* in **a** and **b** 20 μm

embryos with antibodies against cingulin, a specific cytoplasmic TJ protein, reveals diffuse labeling of the maternal protein in the apical cortex (Fig. 1o–p), and accumulation of labeling precisely at the border between new and old membrane, e.g. where JC form, both before (arrow in Fig. 1p) and after sealing (double arrows in Fig. 1p) (see also Cardellini et al. 1996).

Ultrastructural characterization of junctional crests (JC), triple points and junctional vesicles (JV)

We used SEM analysis of intact (Fig. 2a) and fractured embryos (Fig. 2b–e) to examine the morphology of the membrane surface and JC. In the animal pole, the deepening cleavage furrow induces an array of folds and creases in the superficial cortex, tangential to the plane of the contracting ring (insets in Fig. 2a and b, see also Fig. 1c). As new membranes are formed, the cleavage furrow extends vertically towards the center of the egg, and at the same time it broadens laterally, until it encircles the egg, when the two sides converge at the vegetal pole (Fig. 2b). Only at this time is the cleavage furrow complete. The superior part of the furrow, in the animal pole, is closer to the center of the egg and moves towards the bottom, whereas the bottom part of the furrow, in the vegetative pole, pushes upwards. This movement progressively squeezes the cytoplasmic bridge connecting the two blastomeres, thereby reducing its size (asterisk, compare Fig. 2b,c and d). However, a cytoplasmic bridge of about 100 μm diameter is still detectable when the cleavage furrow of the second division has formed (asterisk in Fig. 2c), due to the fact that the cleavage furrow in the vegetal pole advances more slowly than in the animal pole. The cytoplasmic bridge will disappear only when the second cleavage has been completed. When observing the inner surface of fractured 2-cell embryos, the folds induced by the contracting cleavage furrow terminate at a superficial structure, which is more clearly visible in the animal pole (arrows in Fig. 2c). Since this structure separates the morphologically distinguishable old (apical) and new (lateral) membranes (see also Fig. 3), we conclude that this structure corresponds to the JC identified by time-lapse video microscopy. The position of the JC in 2-cell embryos is deep, ~200–300 μm from the external surface of the embryo (Fig. 2b,c), in agreement with the conclusion that early *Xenopus* TJ are located in a deep, recessed position (Merzdorf et al. 1998). As cell division progresses and new lateral membrane is added by exocytosis, the JC appears to move from this deep, internal position to a more external, superficial position (compare Fig. 2c to d). The initial formation of the blastocoel, as a cavity in the center of the embryo, is also visible in fractured embryos analyzed by by SEM (arrow Fig. 2e). A "triple point", where the junction between blastomeres undergoing the second division intersects the junction between the blastomeres resulting from the first cell division, is seen just above the blastocoel (arrow in Fig. 2f). The triple point defines the site where sealing of TJ begins, thus resulting in the separation of the blastocoel from the outside environment. Figure 2g summarizes schematically the events occurring during the first cell division. As the cleavage furrow progresses, the diameter of the cytoplasmic bridge decreases, whereas the surface of the new lateral membrane increases. The JC starts in a narrow apical region, and separates old (apical) from new (lateral) membranes. The JC extends laterally and towards the vegetal pole of the embryo, until it fully encircles the embryo, when the second cell division is already underway.

To characterize JC in further detail, we examined at higher magnification the membrane morphology by SEM (Fig. 3). The old apical membrane and the new lateral membrane are clearly distinct (see also Muller and Hausen 1995). The apical membrane (Ap. in Fig. 3a) displays deeply invaginated folds and abundant surface protrusions, whereas the basolateral membrane (Bas. in Fig. 3a) has fewer, longer protrusions, and displays exocytic pits (Danilchik et al. 2003) (arrowheads in Fig. 3a–g). In a 2-cell embryo, the sealing of JC begins in the apicalmost region of the animal pole, and then propagates laterally and downwards, in a wave-like fashion (boxed areas in Fig. 2c, corresponding to Fig. 3a–d). Thus, by examining the morphology of the JC along its length, it is possible to infer the dynamics of its formation. The areas of the JC which have sealed first lie most proximal to the groove of the second division in the animal pole (Fig. 3a). In this area, the JC is characterized by a linear array of fractured membrane vesicles (arrows in Fig. 3a–d) located precisely at the border between apical and basolateral membranes (Ap. and Bas. in Fig. 3a). We call these vesicles junctional vesicles (JV). The morphology of the fractured JC is not uniform, but its features (fractured JV and villiform protrusions) become progressively less conspicuous going from the animal towards the vegetal pole (arrows in Fig. 3a–d). This is probably due to the fact that adhesion is incomplete towards the vegetal pole, and fractured JV are seen only in areas where the membranes of adjacent blastomeres are adhering more tightly. The different morphology of the fractured JC along the animal–vegetal pole may also reflect a delay in targeting membrane vesicles to the membrane, due to the different composition and density of the cytoplasm along the animal–vegetal axis. In summary, the spatio-temporal correlation between the directional sealing of JC, as assessed by time-lapse video microscopy, and the density of cleaved JV, as assessed by SEM, indicates that junction formation is associated with the intimate apposition of JV to the adhering plasma membranes.

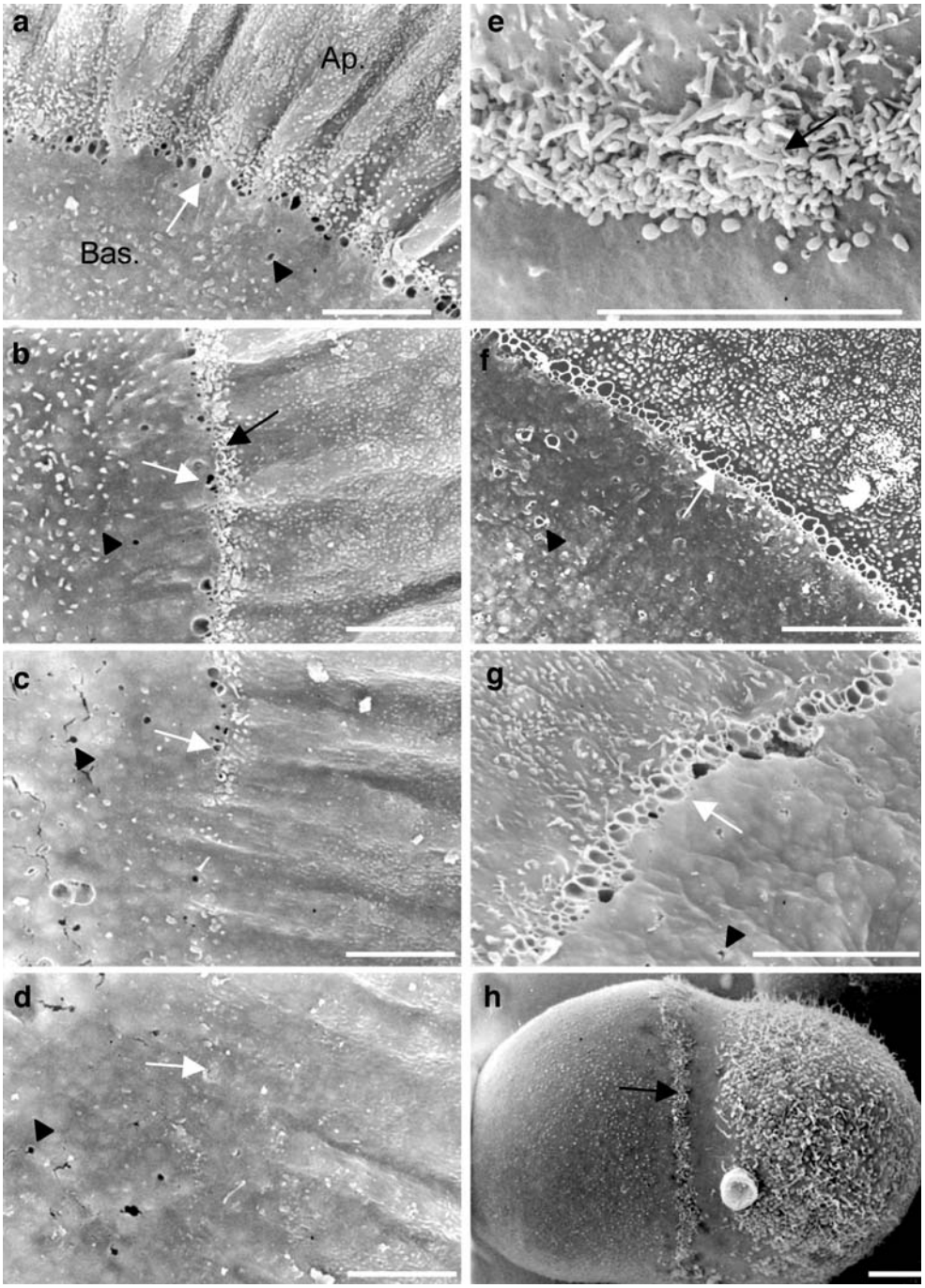

Fig. 3 Scanning electron microscopy analysis of JC. **a**–**d** JC between blastomeres resulting from the first cell division (higher magnification images of boxed areas in Fig. 2c). **e** JC just before the sealing phase in a 32-cell embryo. Note the presence of a dense array of microvillar protrusions. Vesicles are not visualized, since the membranes of adjacent blastomeres have not sealed yet, but we speculate that vesicles are present under the membrane. **f**, **g** Fractured JC between blastomeres of 32-cell embryos. Note the dense array of JV at the border between new and old membrane. **h** Isolated blastomere from an embryo reared in calcium-depleted medium, showing the JC (*arrow*), flanked by apical oolemma (*left*) and new lateral membrane (*right*). *Arrows* in **a**–**g**) indicate fractured JV, whereas *arrowheads* indicate exocytic fusion pores. *Bars* 20 μm

The morphological characteristics of JC are more apparent at later developmental stages. For example, at the 32-cell stage, before sealing, the JC appears as a ~10 μm-thick linear array of microvilli-like protrusions of the plasma membrane (Fig. 3e). Upon sealing of membranes and fracturing of adherent blastomeres, the JC appear as a linear array of tightly packed, fractured vesicles, with diameters ranging between 1 μm and 3 μm (Fig. 3f,g). When embryos are reared in low calcium medium, the JC on adjacent blastomeres do not adhere together, and remain visible as an array of protrusions, which persist at the border between apical and lateral membranes (arrow in Fig. 3h).

Junctional vesicles are associated with ultrastructurally recognizable TJ

To characterize the morphology of JV in further detail, we examined semi-thin and thin sections by light microscopy, TEM, and freeze-fracture. Symmetrically arranged JV of 1–3 μm diameter were detected on each side of the

membranes of adjacent blastomeres (white arrows in Fig. 4a–d)(see also (Kalt 1971b; Cardellini and Rasotto 1988). JV were located near the apicalmost area of the region of contact between adjacent blastomeres, at a distance of about 200 μm from the furrow base (Fig. 4a). When observed at higher magnification, JV were positioned precisely at the border between the apical cortical cytoplasm, rich in pigment granules, and the cytoplasm underlying the lateral membrane, that contained few pigment granules (Fig. 4b,c). In tangential sections, an array of linearly arranged JV, similar to the array observed by SEM, could be observed (Fig. 4c). The presence of pigment granules in the lateral cytoplasm is probably due to the dragging of cortical cytoplasm (cortical ingression) induced by the contracting actomyosin ring. Because of their size and localization, we conclude that these vesicles correspond to the JV identified by SEM analysis of fractured embryos.

To determine whether ultrastructurally recognizable TJ could be detected at JV or in their proximity, samples were

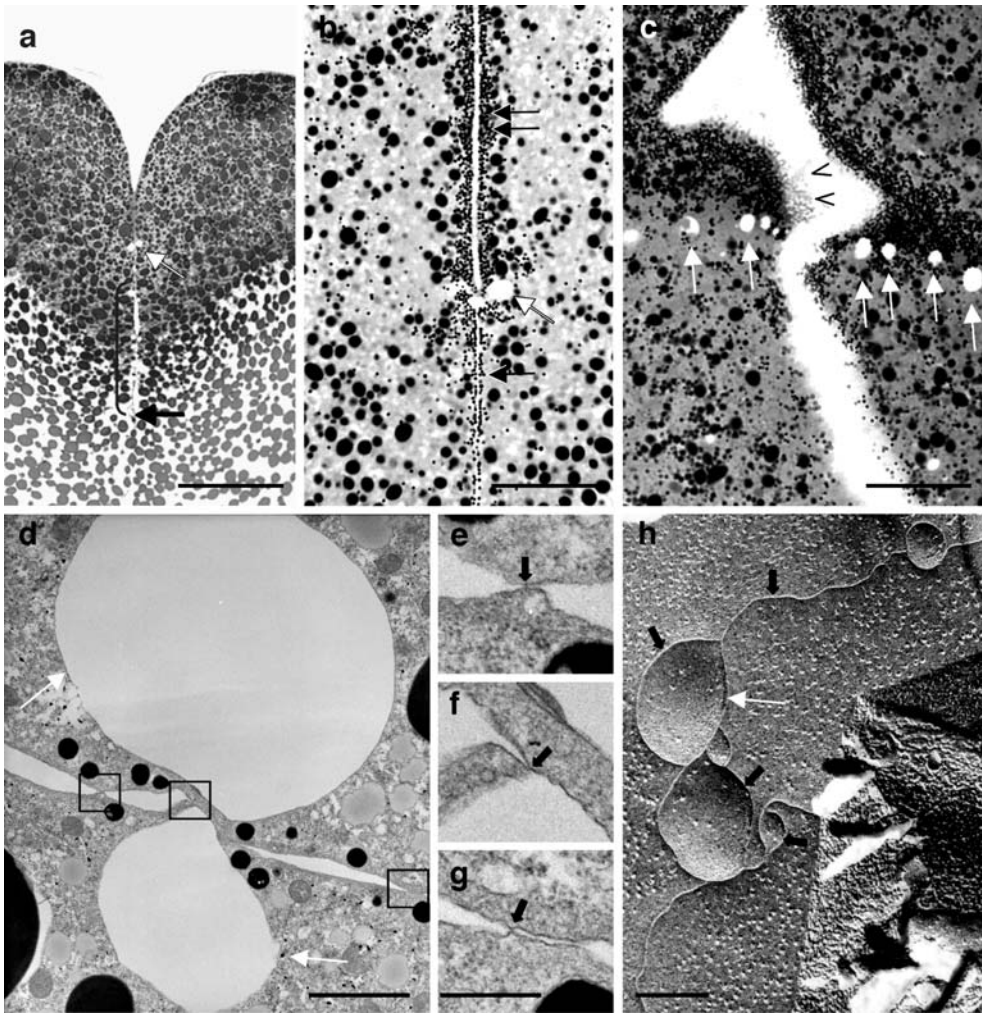

Fig. 4 Morphological analysis JC region and JV by light microscopy (**a**–**c**), TEM (**d**–**g**) and freeze-fracture electron microscopy (**h**). **a**–**c** 1-μm sections of embryos stained with toluidine blue. The section in **c** shows a tangential view of JC, allowing visualization of aligned JV. **d** JV (*white arrows*) and nearby junctional regions, observed by TEM. Note that the bottom JV does not have a continuous border, since its lumen is in direct contact with the plasma membrane of the adjacent blastomere, separated by two junctional regions (one of which is magnified in **f**). **e**–**g** Higher magnification details of the *boxed areas* in **d**. *White arrows* in **a**–**d** indicate JV on the cytoplasmic faces of JC. *Black arrow* in **a** indicates the furrow base. The *bracketed area* in **a** indicates the region of insertion of exocytic vesicles apical to the furrow base. *Double* and *single black arrows* in **b** and **c** indicate pigment granules beneath the plasma membrane, apically and basally, respectively, with respect to JV. Note that the density of the pigment granules is considerably decreased basal to JV, confirming that JV are localized at the fence separating apical from lateral membranes. *Arrowheads* in **c** indicate protrusions in the plasma membrane, apical to the region containing JV. *Black arrows* in **e**–**g** indicate points of apparent focal fusion between plasma membranes of adjacent blastomeres, near JV. *Black arrows* in **h** indicate TJ-like fibrils. *White arrow* in **h** indicates a depressed pit, which we speculate is the result of the fusion and collapse of a JV into the plasma membrane. *Bars*= 30 μm (**a**), 20 μm (**b**, **c**) 1 μm (**d**), 0.2 μm (**e**–**g**), 2 μm (**h**)

analyzed by TEM and freeze-fracture. In thin sections, symmetrically arranged JV on adjacent blastomeres were detected (Fig. 4d). Typically, JV appeared separated from the plasma membrane by a thin cytoplasmic strip (Fig. 4d, top JV). However, very rarely we could observe a JV whose lumen was in direct contact with the plasma membrane of the adjacent blastomere, and separated from the extracellular space by junctions (Fig. 4d, bottom JV). When these junctions, and nearby areas of close contact between the apposed plasma membranes, were analyzed at higher magnification, we could observe points of apparent fusion between the membranes, which obliterated the extracellular space (black arrows in Fig. 4e–g, magnifications of the boxed areas in Fig. 4d). This appearance was highly suggestive of the characteristic "kiss" appearance of sectioned TJ. When the junctional area was subjected to freeze-fracture, continuous intramembrane fibrils were detected around depressed circular pits, and extended along the membrane, to link to nearby pits (black arrows in Fig. 4h) (see also Cardellini and Rasotto 1988), suggesting that TJ fibrils form at sites of fusion of JV with the plasma membrane, when JV collapse into the membrane.

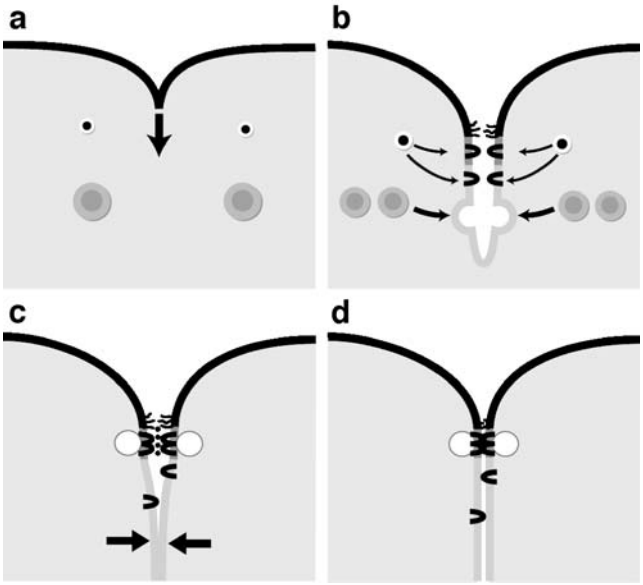

Fig. 5 Schematic diagram of TJ formation during early divisions of a *Xenopus* embryo. Note that different elements are not drawn to scale. **a** When the cleavage furrow forms, membrane vesicles of different sizes, some of which are immunolabeled by antibodies against TJ proteins (Fesenko et al. 2000), are already present in the egg. **b** During the "waiting" phase, the new lateral membrane expands by exocytic fusion of membrane vesicles, many of which (larger, grey vesicles in **b**) are targeted in a microtubule-dependent process to a site about 50 μm from the furrow base (Danilchik et al. 2003). This results in the delivery of TJ proteins (membrane proteins schematically represented as loops inserting twice into the membrane) to the new membrane. **c** Cadherin-dependent cell-cell adhesion brings together the membranes of adjacent blastomeres (*arrows* in **c**). TJ proteins accumulate at the border between old and new membrane, which is characterized by protrusions. We speculate that membrane vesicles are already present on the cytoplasmic face of JC at this stage. **d** The JC on adjacent blastomeres seal together, thus creating a paracellular barrier and sealing the extracellular space. Sealed JC are characterized by the presence of symmetrically located JV closely apposed to the cytoplasmic face of the junction, as shown by SEM and TEM. Note that although TJ proteins such as occludin are accumulated at apicolateral TJ, they are still detected along the lateral membrane (Fesenko et al. 2000; Chalmers et al. 2003)

Discussion

We used time-lapse video microscopy, SEM, TEM and freeze-fracture to obtain new evidence about the dynamics of junction formation, the morphology of junctional membranes, and TJ biogenesis in early cleavages of *Xenopus* embryos. Our results indicate that formation of TJ occurs following the sealing of JC, which are characterized by villiform protrusions and by symmetrically located JV. Figure 5 summarizes schematically our model for TJ formation during *Xenopus* early cleavages. When the embryo starts to divide, maternally provided TJ proteins are either associated with the apical cortex (cingulin, aPKC; Cardellini et al. 1996; Fesenko et al. 2000; Chalmers et al. 2003) or with different types of cytoplasmic vesicles (Fesenko et al. 2000) (Fig. 5a). Vesicles containing either occludin or ZO-1 are targeted to the lateral membrane through exocytic fusion (Fig. 5b). The apicalmost regions of the lateral membranes seal together in a process that requires cadherin activity, and which may be mediated by interaction of villiform protrusions of JC (Fig. 5c). Sealing of JC is associated with the apposition of JV onto the inner surface of the plasma membrane. TJ proteins are accumulated at sites near JV, resulting in the formation of ultrastructurally recognizable TJ (Fig. 5d). Eventually, JV will collapse into the membrane and disappear.

TJ can be identified by a variety of criteria. Ultrastructurally, by the presence of points of apparent fusion of the external leaflets of the plasma membrane in sectioned samples ("kisses"), and by fibrils in freeze-fractured samples. Functionally, by their topological association either with the boundary between different plasma membrane domains (fence function), and/or with the sites of blockage to the paracellular diffusion of a detectable tracer (barrier function). Molecularly, by the immunolocalization of specific TJ proteins. Here, we used TEM to show that ultrastructurally recognizable TJ are associated with JV. In addition, TJ-like fibrils were detected near circular areas of depressed membrane, which we speculate may result from the fusion and collapse of JV into the plasma membrane. We also used the functional fence criterium, since TEM analysis showed that JV were located at the boundary between pigment-rich apical membrane domain, and pigment-poor

lateral membrane domain. In addition, both light microscopy and SEM analysis showed that JC were localized at the border between membrane domains, whose surfaces were morphologically distinct. Importantly, the border between pigmented apical membrane and non-pigmented lateral membrane is also the site where the TJ-specific protein cingulin is accumulated (Cardellini et al. 1996) (molecular criterium), and also corresponds precisely to the point where biotin diffusion is blocked by the TJ barrier, starting from stage 1st/360° (Fesenko et al. 2000) (functional barrier criterium). Taken together, these data indicate that in early *Xenopus* embryogenesis functional TJ form following the sealing of JC, at sites containing JV. The notion that cingulin is localized at TJ was challenged by Merzdorf et al. (1998) who observed deep penetration of biotin in early *Xenopus* embryos. However, Merzdorf et al. (1998) did not simultaneously immunolocalize any TJ protein, and the deeper penetration of biotin observed in their 2-cell embryos could have been due to a transient leakage of biotin. Indeed, we later showed that biotin can still diffuse to the lateral spaces, past TJ, between the 1st/90° and the 1st/360° stages of cleavage, at a time when the TJ fence is already established (Fesenko et al. 2000). Only after the 1st/360° stage is a functional barrier to biotin formed, and the site where biotin is blocked corresponds precisely to the "fence" site where cingulin, occludin and ZO-1 accumulate (Fesenko et al. 2000).

Time-lapse analysis indicated that the formation of JC is preceded by a "mixing" phase, when an apparent transient mixing of unpigmented and pigmented membranes occurs. We speculate that this phase is due to some reorganization of the cytoskeleton-membrane interface, which occurs prior to the emergence of JC. JC are formed even in the absence of cadherin-mediated adhesion, but under these circumstances they do not seal, and persist as an array of villiform protrusions. We speculate that villiform projections of JC are poised to link with their opposite number, and they could be formed either as a result of exocytic fusion of membrane vesicles, or a localized process of actin polymerization (Vasioukhin and Fuchs 2001). Future studies should investigate the molecular composition of these protrusions and what defines their topogenesis. Under normal calcium conditions, the JC rapidly seal in a zipper-like, directional fashion, starting from the side closest to the junction formed in a previous cell division. This side corresponds to the location of a tricellular contact ("triple point"), which we described here by light microscopy and SEM. It is noteworthy that a new transmembrane protein, tricellulin, was recently identified, which localizes exclusively at points of tricellular contacts in MDCK cells, and plays a role in the TJ barrier function (Ikenouchi et al. 2005).

The lateral membrane, below the JC, is generated by microtubule-dependent exocytotic fusion of membrane vesicles, which results in the appearance of exocytic pits on the outside surface of the membrane (Fig. 3; see also Danilchik et al. 2003). Based on their size and localization, we believe that the vesicles labelled by anti-ZO-1 antibodies, that we identified in sections of *Xenopus* embryos by immunofluorescence (Fesenko et al. 2000), belong to this subset of vesicles and are distinct from JV. Additional vesicles, including those labelled by anti-occludin antibodies (Fesenko et al. 2000), which are smaller and thus also distinct from JV, also fuse into the new lateral membrane by exocytosis, at apparently more random locations (Fig. 5). The fusion of exocytotic vesicles results in an expansion of the surface of the new membrane, and the delivery of proteins, which will provide the material for building cell-cell junctions.

The biogenesis, molecular composition and membrane targeting of JV remain to be clarified. Although components of the exocyst complex have been shown to be associated with junctional proteins during polarization of vertebrate epithelial cells (Grindstaff et al. 1998; Yeaman et al. 2004), there is no evidence for the localization of components of the exocyst or SNARE complexes at *Xenopus* cell–cell junctions. However, a special type of exocytosis, named "kiss-and-coat" exocytosis, has been described in frog and fish eggs, where large vesicles (0.5–3 μm) coated by actin filaments remain associated with the plasma membrane for prolonged periods without collapsing into the plasma membrane (Sokac and Bement 2006). Such vesicles could represent a portal for subsequent fusion events with smaller vesicles, or retrieval of membrane by endocytosis. We propose that JV may be a type of "kiss-and-coat" exocytic vesicles, and represent sites where TJ proteins are recruited, sorted and enriched from the apical cortex (e.g. cingulin, aPKC), the adjacent lateral membrane (e.g. ZO-1, occludin, claudins) or fusing vesicles. This could lead to their accumulation, polymerization and stabilization through cytoskeletal interaction, resulting in the formation of ultrastructurally recognizable TJ fibrils. We speculate that eventually the membranes of JV fuse with the plasma membrane and JV collapse into the plasma membrane, as suggested by our TEM and freeze-fracture observations (Fig. 4).

In summary, our previous studies demonstrate that TJ form at one site at the boundary between apical and lateral membranes, where TJ proteins accumulate, and a functional block to biotin permeability is generated. Here, we describe the dynamics of the formation of such boundary region, and we characterize its morphology by SEM, TEM, and freeze-fracture, showing that it contains ultrastructurally recognizable TJ. The identification of JV raises the hypothesis that TJ assembly could be associated with a form of "kiss-and-coat" exocytosis, and prompts further studies on the molecular nature of these vesicles, and the signaling pathways implicated in their biogenesis.

References

Bluemink JG (1971) Effects of cytochalasin B on surface contractility and cell junction formation during egg clevage in *Xenopus laevis*. Cytobiologie 3:176–187

Byers TJ, Armstrong PB (1986) Membrane protein redistribution during *Xenopus* first cleavage. J Cell Biol 102:2176–2184

Cardellini P, Rasotto MB (1988) Intercellular connections in *Xenopus laevis* egg at the 8-cell stage. Acta Embryol Morphol Exp 9:97–103

Cardellini P, Davanzo G, Citi S (1996) Tight junctions in early amphibian development: detection of junctional cingulin from the 2-cell stage and its localization at the boundary of distinct membrane domains in dividing blastomeres in low calcium. Dev Dyn 207:104–113

Chalmers AD, Strauss B, Papalopulu N (2003) Oriented cell divisions asymmetrically segregate aPKC and generate cell fate diversity in the early *Xenopus* embryo. Development 130:2657–2668

Danilchik MV, Bedrick SD, Brown EE, Ray K (2003) Furrow microtubules and localized exocytosis in cleaving *Xenopus laevis* embryos. J Cell Sci 116:273–283

Farquhar MG, Palade GE (1963) Junctional complexes in various epithelia. J Cell Biol 17:375–412

Fesenko I, Kurth T, Sheth B, Fleming TP, Citi S, Hausen P (2000) Tight junction biogenesis in the early *Xenopus* embryo. Mech Dev 96:51–65

Goodenough DA, Revel JP (1970) A fine structural analysis of intercellular junctions in the mouse liver. J Cell Biol 45:272–290

Grindstaff KK, Yeaman C, Anandasabapathy N, Hsu SC, Rodriguez-Boulan E, Scheller RH, Nelson WJ (1998) Sec6/8 complex is recruited to cell-cell contacts and specifies transport vesicle delivery to the basal-lateral membrane in epithelial cells. Cell 93:731–740

Ikenouchi J, Furuse M, Furuse K, Sasaki H, Tsukita S, Tsukita S (2005) Tricellulin constitutes a novel barrier at tricellular contacts of epithelial cells. J Cell Biol 171:939–945

Kalt MR (1971a) The relationship between cleavage and blastocoel formation in *Xenopus laevis*. I. Light microscopic observations. J Embryol Exp Morphol 26:37–49

Kalt MR (1971b) The relationship between cleavage and blastocoel formation in *Xenopus laevis*. II. Electron microscopic observations. J Embryol Exp Morphol 26:51–66

Merzdorf CS, Chen YH, Goodenough DA (1998) Formation of functional tight junctions in *Xenopus* embryos. Dev Biol 195:187–203

Muller HA, Hausen P (1995) Epithelial cell polarity in early *Xenopus* development. Dev Dyn 202:405–420

Palmer JF, Slack C (1970) Some bio-electric parameters of early *Xenopus* embryos. J Embryol Exp Morphol 24:535–553

Sanders EJ, DiCaprio RA (1976) Intercellular junctions in the *Xenopus* embryo prior to gastrulation. J Exp Zool 197:415–421

Sanders EJ, Singal PK (1975) Furrow formation in *Xenopus* embryos. Involvement of the golgi body as revealed by ultrastructural localization of thiamine pyrophosphatase activity. Exp Cell Res 93:219–224

Sanders EJ, Zalik SE (1972) The blastomere periphery of *Xenopus laevis*, with special reference to intercellular relationships. Wilhelm Roux' Arch Entwicklungsmech Org 171:181–194

Slack C, Warner AE (1973) Intracellular and intercellular potentials in early amphibian embryo. J Physiol 232:313–330

Sokac AM, Bement WM (2006) Kiss-and-coat and compartment mixing: coupling exocytosis to signal generation and local actin assembly. Mol Biol Cell 17:1495–1502

Tsukita S, Furuse M, Itoh M (2001) Multifunctional strands in tight junctions. Nat Rev Mol Cell Biol 2:285–293

Vasioukhin V, Fuchs E (2001) Actin dynamics and cell-cell adhesion in epithelia. Curr Opin Cell Biol 13:76–84

Yeaman C, Grindstaff KK, Nelson WJ (2004) Mechanism of recruiting Sec6/8 (exocyst) complex to the apical junctional complex during polarization of epithelial cells. J Cell Sci 117:559–570